LIGHT SATURATION CURVES AND QUANTUM YIELDS IN REACTION CENTERS FROM PHOTOSYNTHETIC BACTERIA

HERMAN M. CHO, L. J. MANCINO, AND ROBERT E. BLANKENSHIP
Department of Chemistry, Amherst College, Amherst, Massachusetts 01002

ABSTRACT   Reaction centers isolated from the photosynthetic bacterium *Rhodopseudomonas sphaeroides* R-26 mutant were irradiated with laser pulses of variable energy and the amount of photooxidation of the primary electron donor bacteriochlorophyll was measured. The resultant light saturation curve fits an exponential function and not a hyperbolic or hyperbolic tangent function. Analysis using either a Poisson statistical model or a simple kinetic model predicts an exponential light saturation curve in the limit where the light pulse is long relative to any transient intermediate states. The absolute quantum yield of photochemistry was found to be 0.98, utilizing the entire light saturation curve. Distortions from the simple exponential light saturation behavior are predicted when very short laser pulses are used.

INTRODUCTION

The measurement of light saturation curves has long been a fruitful experiment in research into the mechanism of photosynthesis. Blackman (1) correctly interpreted the characteristic shape of continuous light saturation curves in terms of a photochemical reaction followed by a dark reaction, and the classic flash saturation experiments of Emerson and Arnold (2) established the concept of the photosynthetic unit. The low intensity or light limiting region of the light saturation curve serves as a measure of the maximum quantum yield of the photochemical process. The rate in saturating continuous light reflects the maximum rate of the dark reactions that follow the photochemical step, while the maximal yield from a saturating flash reflects the number of active photosynthetic centers. The precise shape of the photosynthetic light saturation curve has been the subject of much debate (see Rabinowitch [3] for a review of the early literature).

Many continuous light experiments are described well by a hyperbolic equation, undoubtedly reflecting the enzymatic nature of the dark reactions. It has often been assumed in analogy to the well-known hyperbolic shape of V_{max} vs. substrate plots of many enzymatic reactions that saturation curves from flash-induced experiments are also hyperbolic in shape. However, Emerson and Arnold (2) fit their original data using an exponential function, and the analogy to substrate saturation curves in enzymatic reactions is a weak one.

Recently, Mauzerall, and co-workers have used statistical arguments to explain flash saturation data in photosynthetic systems (4–7). Their analysis predicts that flash saturation curves for photochemistry should be essentially exponential, although heterogeneity in the antenna system can affect the predicted shape somewhat.

Most absolute quantum yield measurements on photosynthetic systems have been performed on living algae or bacteria (3). While these measurements are invaluable in determining overall photosynthetic efficiency, complications due to respiratory activity and antenna processes make them somewhat less useful in probing the primary photochemical act. Relatively few absolute quantum yield measurements have been made on subcellular preparations. The experiments of Loach and Sekura (8) on bacterial chromatophores and Wraight and Clayton (9) on isolated bacterial reaction centers both resulted in absolute quantum yield values near unity. While we have no reason to doubt the validity of these careful measurements, the reversible nature of the photochemistry in photosynthetic systems poses special experimental problems for quantum yield determinations and restricts the applicability of the initial rate methods used. In particular, if the recombination rate varies from sample to sample, as is observed in quinone-depleted reaction centers reconstituted with artificial acceptors (10, 11), the continuous-light method is extremely difficult.

In this work we have investigated the intrinsic shape of the flash-induced light saturation curve for bacteriochlorophyll oxidation in isolated reaction centers from photosynthetic bacteria and have found it to be exponential. We have used these light saturation curves to determine absolute quantum yields of photochemistry in reaction centers.

Dr. Cho's present address is the Department of Chemistry, University of California, Berkeley, California 94720.
Correspondence should be addressed to Dr. Blankenship.

This technique utilizes the entire light saturation curve to determine the intrinsic quantum yield, and is well suited for quantum yield measurements in many reversible photochemical systems since it is insensitive to the recombination rate of the system over a wide range.

MATERIALS AND METHODS

Reaction Center Preparation and ϵ Determination

Reaction centers were isolated from cells of *Rhodopseudomonas sphaeroides* R-26 mutant essentially as described in reference 12. The extinction coefficient at the laser wavelength was measured by filtering a sample of reaction centers in 0.1% lauryl dimethylamine oxide (gift of Onyx Chemical Co., Jersey City, NJ), 10 m M Tris, pH 8.0, 10 μM EDTA through a 0.2-μ filter to remove particulates and by recording an absorption spectrum on a Cary 219 spectrophotometer (Varian Associates, Inc., Palo Alto, CA) interfaced to an Apple II + computer (Apple Computer Inc., Cupertino, CA). The extinction coefficient at 802 nm of 288 ±14 mM^{-1}cm^{-1} measured by Straley et al. (13) was used to calculate the extinction coefficient at 583.5 nm of 51.5 ± 3 mM^{-1}cm^{-1}.

Laser-induced Absorbance Change Measurements

Flash-induced absorbance change measurements were made on a home-built single beam spectrophotometer. Laser pulses of 1-μs duration, 1-J energy, and 583.5-nm wavelength were obtained from a flashlamp-pumped dye laser (model SLL-625; Candela Corp., Natick, MA). An optical flat oriented at 45° to the beam axis split out ~10% of the pulse for intensity measurements, while the remainder passed through calibrated neutral density filters and impinged on the 5-mm side of a 5 × 10-mm glass cuvette. Beam profile measurements indicated that the pulse had a flat-topped intensity vs. position profile rather than a Gaussian profile. This resulted from gain saturation of the dye (3 × 10^{-5} M Exciton rhodamine 590 tetrafluoroborate in methanol; Exciton Chem. Corp., Dayton, OH) and provided essentially even illumination across the front surface of the cuvette. The laser wavelength was measured as 583.5 nm using a scattering sample, photomultiplier, and an H-20 monochromator (Instruments S. A., Inc., Metuchen, NJ). The monochromator was calibrated using a HeNe laser.

A 100-W tungsten halogen lamp operated with a stabilized (DC) power supply served as a measuring light source. After wavelength selection with a 3-69 filter (Corning Glass Works, Corning, NY) and an H-20 monochromator (Instruments S. A., Inc.), the beam traversed the cuvette at a right angle to the laser pulse. The measuring beam was masked so that it probed only the region of the sample that was evenly illuminated by the laser pulse. A monochromator (H-10; Instruments S. A., Inc.) and 720-nm long pass filter provided rejection of scattered laser light. The intensity of the measuring beam was measured by a UDT-455 photodiode-amplifier (United Detector Technology, Santa Monica, CA), and the kinetic trace was recorded on an Explorer III digital oscilloscope (model 206; Nicolet Instrument Corp., Madison, WI) with a 12 bit resolution analog-to-digital plug-in. The trace was then transferred to a computer (9825-B; Hewlett-Packard Co., Palo Alto, CA) and stored on magnetic tape for later analysis. A sequence of 54 single flash measurements was performed, beginning with weak flashes, proceeding up to full intensity flashes, and back down to weak flashes. No irreversible photochemical effects were observed.

Light Intensity Measurements

The absolute intensity of laser flashes in photons cm^{-2} incident on the cuvette front surface was measured by positioning a Scientech 360001 joulemeter with a model 362 power/energy readout (Scientech Inc.,

Boulder, CO) in place of the cuvette. The laser pulse was centered on a 3/16" diam pinhole at the entrance to the joulemeter and the energies of 15 laser pulses were individually measured. The joulemeter was then moved so as to measure the portion of the pulse deflected by the beamsplitter, the pinhole was removed, and the energies of 15 pulses were individually measured. This process was repeated several times, so that a proportional relationship between the total pulse intensity and the energy of the central portion was established. The excellent pulse-to-pulse stability of the laser output energy (1–2%) and uniform spatial energy distribution, as judged by the perfectly round burn spots on Polaroid film facilitated this determination. A set of neutral density filters (No. 5076; Oriel Corp. of America, Stamford, CT) was calibrated at 583.5 nm using Cary 15 and 219 spectrophotometers (Varian Associates, Inc.) and was used to attenuate the laser output. A small correction for sample absorption and reflection from the cuvette faces was applied as described in Appendix I.

Data Analysis

The raw data were converted from transmittance to absorbance and a weighted semilog least-squares fit was performed to determine the absorbance change induced by the laser flash. A set of 54 ΔA vs. I pairs were obtained in this manner and were transferred to a VAX 11/780 (Digital Equipment Corp., Marlboro, MA) and fit using a nonlinear least-squares routine based on Newton's method (14).

RESULTS

Experimental

Typical raw data traces of laser flash-induced transmittance changes at 865 nm at six different flash intensities are shown in Fig. 1, illustrating the phenomenon of light saturation. A bleaching of the 870-nm absorption band in reaction centers from purple photosynthetic bacteria occurs when the primary electron donor bacteriochlorophyll, P870, is oxidized. This photooxidation occurs on a picosecond time scale, and reverses to the preflash state with a first-order rate constant of 10 s^{-1} in reaction centers with a single molecule of ubiquinone (UQ) as electron acceptor. The state monitored in these experiments is P870$^+$UQ$^-$, the first charge separated state of bacterial photosynthesis that is stable for longer than a few nanoseconds. Earlier charge separated states are known to exist in the system; the precursor to the P870$^+$UQ$^-$ state is P870$^+$BPheo$^-$, where BPheo is one of the two bacteriopheophytin molecules that are present in the reaction center complex (15).

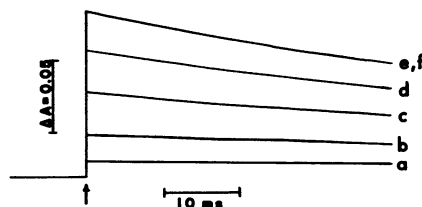Complete light saturation curves are shown in Fig. 2.

FIGURE 1 Laser–flash-induced transmittance changes at 865 nm in isolated reaction centers. The arrow indicates when the laser pulse occurs. Curves *a–f* are the results of laser pulses at 5.66 × 10^{14}, 1.59 × 10^{15}, 3.82 × 10^{15}, 8.00 × 10^{15}, 8.50 × 10^{16}, and 8.87 × 10^{17} photons cm^{-2}.
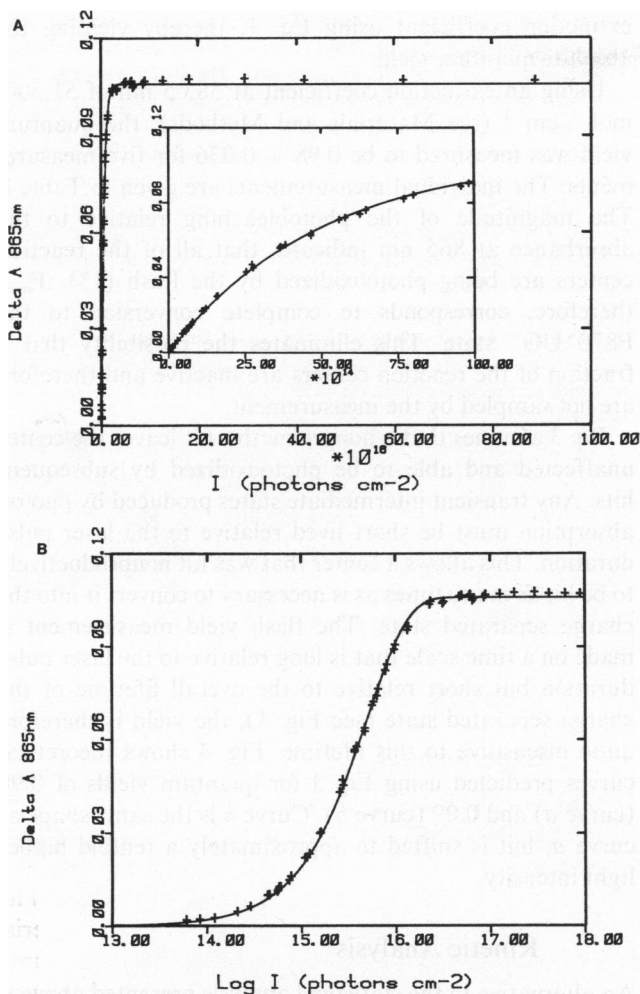
FIGURE 2 Flash saturation curves from isolated reaction centers. *A*, Linear scale. *B*, Logarithmic scale. The *inset* in *A* is an expansion of the lowest 1% of the intensity scale of *A*. The solid line (——) in all cases is the least-squares fit to an exponential function.

FIGURE 3 Comparison of three different fitting functions for flash saturation curves. *A*, +, experimental points; ——, fit to the exponential equation $\Delta A = \Delta A_{max} (1 - \exp(-\sigma E\Phi))$; (---), fit to the hyperbolic equation $\Delta A = \Delta A_{max} E/(K + E)$; (---), fit to the hyperbolic tangent equation $\Delta A = \Delta A_{max} \tanh(KE)$. *B*, Residuals of the fits. +, exponential; x, hyperbolic; o, hyperbolic tangent.

The traditional linear intensity plot is shown in Fig. 2 *A*, with the low intensity region expanded in the inset. The same data are replotted on a logarithmic intensity scale in Fig. 2 *B*. Since the data span a range of flash energies of nearly five orders of magnitude, the logarithmic plot is a more useful way to present the data and will be used henceforth. The solid line in Fig. 2 is the best-fit exponential function resulting from the nonlinear least-squares fitting procedure described in the Materials and Methods.

Both the Poisson statistical and the kinetic models discussed below predict an exponential shape for the light saturation curve, so the excellent fit of the exponential function to the data of Fig. 2 is as expected. It is of considerable interest, however, to determine if the intrinsic shape of the curve is indeed exponential. To this end nonlinear least-squares fits to the data of Fig. 2, using three different two-parameter functions, are shown in Fig. 3 *A*, with the residuals to each fit shown in Fig. 3 *B*. The exponential function consistently gives the best fits. The
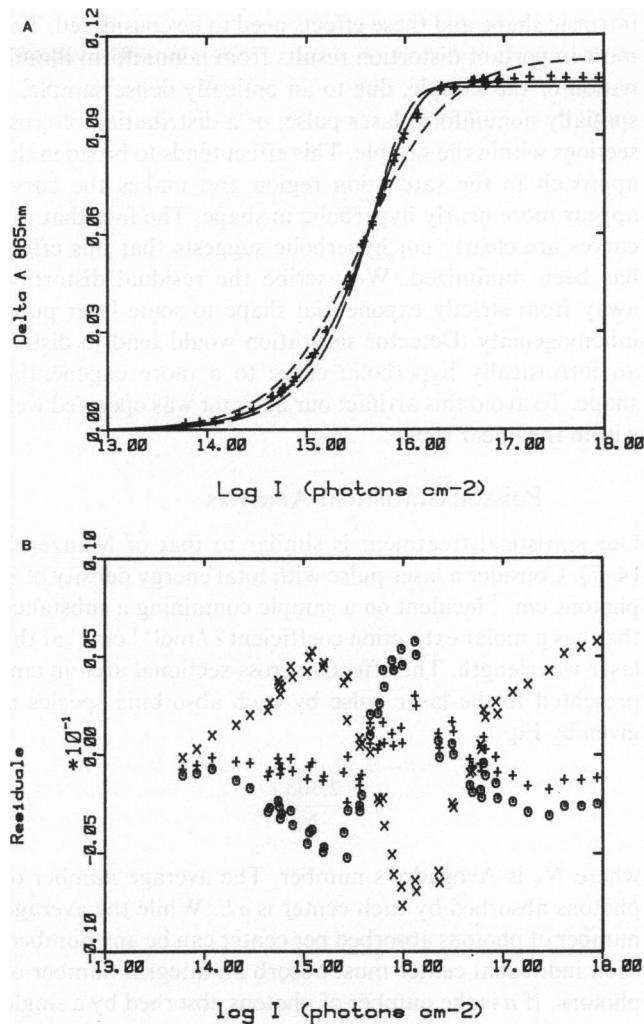
hyperbolic tangent is second best and the hyperbolic function gives the poorest fit to the data. The sums of the residuals of the three fits were compared, and in every one of ten experiments (five with relative and five with absolute intensity measurements), the exponential fit the data most accurately. The F test is the proper way to determine if these differences are statistically significant. Reduced chi squares were compared for the three functions; in all cases the results were significant at the 95% level of confidence (16), and in most cases greatly exceeded this level. This establishes that, of the three functions tested, the exponential fits the data the best.

The results of Fig. 3 clearly indicate that the observed light saturation curve is indeed exponential. Experimental difficulties can, however, lead to a distortion of the observed shape of the light saturation curve away from the

intrinsic shape and these effects need to be considered. The most important distortion results from nonuniform illumination of the sample, due to an optically dense sample, a spatially nonuniform laser pulse, or a distribution of cross sections within the sample. This effect tends to broaden the approach to the saturation region and makes the curve appear more nearly hyperbolic in shape. The fact that the curves are clearly not hyperbolic suggests that this effect has been minimized. We ascribe the residual distortion away from strictly exponential shape to some laser pulse inhomogeneity. Detector saturation would tend to distort an intrinsically hyperbolic curve to a more exponential shape. To avoid this artifact our detector was operated well within the linear range.

Poisson Statistical Analysis

Our statistical treatment is similar to that of Mauzerall (4–7). Consider a laser pulse with total energy density of E photons cm^{-2} incident on a sample containing a substance that has a molar extinction coefficient ϵ l mol^{-1} cm^{-1} at the laser wavelength. The effective cross-sectional area in cm^2 presented to the laser pulse by each absorbing species is given by Eq. 1

$$\sigma = \frac{2,303\,\epsilon}{N_A},\qquad(1)$$

where N_A is Avogadro's number. The average number of photons absorbed by each center is σE. While the average number of photons absorbed per center can be any number, each individual center must absorb an integral number of photons. If n is the number of photons absorbed by a single center (hits), the distribution of hits in the collection of centers is given by the Poisson distribution

$$P_n = \frac{x^n e^{-x}}{n!},\qquad(2)$$

where x is the average number of hits to each center. $P_0 = e^{-x}$ is the fraction of centers that receive no hits, $P_1 = xe^{-x}$ receive one hit, etc. The number of centers that receive at least one hit is $1 - P_0$ or $1 - e^{-x}$. If we now include the possibility that any given hit can either convert the center to the stable charge separated state or leave it effectively unchanged, the relative yield of charge separated states is given by the cumulative one-hit Poisson distribution (4–7)

$$\frac{Y}{Y_{max}} = 1 - e^{-\phi\sigma E},\qquad(3)$$

where the quantum yield ϕ is the probability that a hit will produce the charge separated state. The apparent "decay constant" of the exponential light saturation curves is therefore a product of the quantum yield and a cross-section factor. The cross-section factor is obtained from the

extinction coefficient using Eq. 1, thereby yielding the absolute quantum yield.

Using an extinction coefficient at 583.5 nm of 51,500l mol^{-1} cm^{-1} (see Materials and Methods), the quantum yield was measured to be 0.98 ± 0.036 for five measurements. The individual measurements are given in Table I. The magnitude of the photobleaching relative to the absorbance at 865 nm indicates that all of the reaction centers are being photooxidized by the flash (13). Y_{max}, therefore, corresponds to complete conversion to the $P870^+UQ^-$ state. This eliminates the possibility that a fraction of the reaction centers are inactive and therefore are not sampled by the measurement.

Eq. 3 assumes that a nonproductive hit leaves the center unaffected and able to be photooxidized by subsequent hits. Any transient intermediate states produced by photon absorption must be short lived relative to the laser pulse duration. This allows a center that was hit nonproductively to be hit as many times as is necessary to convert it into the charge separated state. The flash yield measurement is made on a time scale that is long relative to the laser pulse duration but short relative to the overall lifetime of the charge separated state (see Fig. 1); the yield is therefore quite insensitive to this lifetime. Fig. 4 shows theoretical curves predicted using Eq. 3 for quantum yields of 0.98 (curve a) and 0.09 (curve b). Curve b is the same shape as curve a, but is shifted to approximately a tenfold higher light intensity.

Kinetic Analysis

An alternative to the statistical analysis presented above is a kinetic analysis in which one of the rate constants is proportional to light intensity. A simple kinetic scheme that effectively incorporates all the significant kinetic processes operating in isolated reaction centers is shown in Fig. 5 (inset). The rate constant k_{12} is assumed to be light dependent: $k_{12} = \sigma I$, where I is the photon density per unit time in units of photons cm^{-2} s^{-1}. The quantum yield of formation of the charge separated state A_3 is $\phi = k_{23}/(k_{21} + k_{23})$.

TABLE I

Experiment No.	Quantum yield
1	0.90
2	1.02
3	1.01
4	1.07
5	0.89
mean 0.98 ± 0.036	

The quoted uncertainty is the standard deviation of the mean, calculated from $\sigma_m = s/\sqrt{N}$, where s is the standard deviation of the data and N is the number of experiments (16). All experiments with absolute intensity measurements are included.
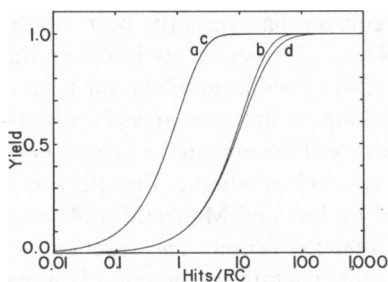
FIGURE 4 Theoretical plots of light saturation curves. a, Eq. 3, $\Phi = 0.98$; b, Eq. 3, $\Phi = 0.091$; c, Eq. 11, pulse duration $= 10^{-6}$ s, $k_{21} = 10^8$ s^{-1}, $k_{23} = 5 \times 10^9$ s^{-1}; d, Eq. 11, pulse duration $= 10^{-6}$ s, $k_{21} = 10^8$ s^{-1}, $k_{23} = 10^7$ s^{-1}.

This kinetic scheme can be solved analytically to yield the populations of the three states at time t after the initiation of the laser pulse (17)

$$A_1(t) = A_1^0 \left[\frac{k_{12} - \lambda_3}{\lambda_2 - \lambda_3} e^{-\lambda_2 t} + \frac{\lambda_2 - k_{12}}{\lambda_2 - \lambda_3} e^{-\lambda_3 t} \right] \quad (4)$$

$$A_2(t) = A_1^0 \left[\frac{-k_{12}}{\lambda_2 - \lambda_3} e^{-\lambda_2 t} + \frac{k_{12}}{\lambda_2 - \lambda_3} e^{-\lambda_3 t} \right] \quad (5)$$

$$A_3(t) = A_1^0 \left[1 + \frac{\lambda_3}{\lambda_2 - \lambda_3} e^{-\lambda_2 t} - \frac{\lambda_2}{\lambda_2 - \lambda_3} e^{-\lambda_3 t} \right], \quad (6)$$

where A_1^0 is the population of A_1 at $t = 0$ ($A_2^0 = A_3^0 = 0$),

$$\lambda_2 = \frac{1}{2}(p + q) \quad (7)$$

$$\lambda_3 = \frac{1}{2}(p - q) \quad (8)$$

and

$$p = k_{12} + k_{21} + k_{23} \quad (9)$$

$$q = [(k_{12} + k_{21} + k_{23})^2 - 4 k_{12} k_{23}]^{1/2}. \quad (10)$$

If the laser pulse is terminated at time t and the metastable state A_2 is allowed to decay completely, the eventual yield of state A_3 is

$$A_3(\infty) = A_3(t) + A_2(t) \frac{k_{23}}{k_{21} + k_{23}}. \quad (11)$$

The first term in Eq. 11 represents A_3 formed during the light pulse, while the second term represents A_3 formed from A_2 after the pulse.

Fig. 4, curves c and d, are plots of Eq. 11 vs. number of hits for a 1-μs laser pulse, $k_{21} = 10^8$ s^{-1}, and $k_{23} = 5 \times 10^9$ s^{-1} (curve c); or 10^7 s^{-1} (curve d). These rate constants correspond to quantum yields of 0.98 and 0.09, respectively. The Poisson curve for $\phi = 0.98$ is superimposable with the exact kinetic result, while the low quantum yield curves deviate slightly at high energies. This reflects a breakdown in the assumption made in deriving the Poisson curve that the pulse length is long relative to the lifetime of the intermediate state. Curves a and c of Fig. 4 clearly
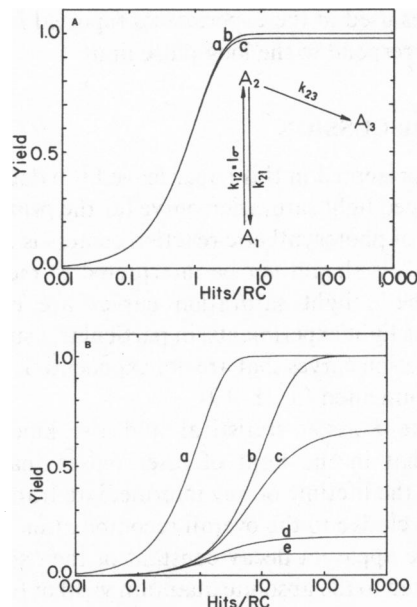

FIGURE 5 Pulse duration dependence of saturation behavior. A, Plots of Eq. 11. All curves calculated with $k_{21} = 10^8$ s^{-1} and $k_{23} = 5 \times 10^9$ s^{-1}. Pulse duration: curve a, 10^{-6} s; curve b, 10^{-9} s; curve c, 10^{-12} s. A, inset equivalent kinetic scheme for bacterial reaction centers. Extremely rapid reactions that follow the primary photochemical reaction have been incorporated into the photochemical step. A_1 corresponds to P870BpheoUQ, A_2 corresponds to P870$^+$Bpheo$^-$UQ, and A_3 corresponds to P870$^+$BpheoUQ$^-$. B, Plots of Eq. 11. Curve a, calculated with $k_{21} = 10^8$ s^{-1}, $k_{23} = 5 \times 10^9$ s^{-1}, and pulse duration $= 10^{-6}$ s. Curves b–e, calculated with $k_{21} = 10^8$ s^{-1} and $k_{23} = 10^7$ s^{-1}. Pulse duration: curve b, 10^{-6} s; curve c, 10^{-7} s; curve d, 10^{-8} s; curve e, 10^{-9} s.

represent the same function. This can easily be verified by examining the appropriate limit of Eq. 11 when $k_{12} \ll k_{21} + k_{23}$.

It is of interest to examine the predictions of the exact kinetic model using a variety of pulse durations and kinetic constants. Under conditions where the photochemical quantum yield is high, the light saturation curve is nearly independent of pulse duration (Fig. 5 A), while under low quantum yield conditions the curves are strongly dependent on pulse duration (Fig. 5 B). In the limit of a very short pulse the relative yield of A_3 at infinite intensity is simply the quantum yield of A_3 formation, and the light saturation curve is described by the function

$$Y/Y_{\max} = \phi(1 - e^{-\sigma E}). \quad (12)$$

In this situation there is no opportunity for the multiple traverses through the reaction cycle that are required to drive the production of A_3 to completion. Pulses of intermediate duration result in light saturation curves with a more complex shape. The pulse duration that corresponds to the short pulse limit is somewhat dependent on the quantum yield and the kinetic constants; under the conditions of Fig. 5 B ($\phi = 0.09$) the short pulse limit is 10^{-9}s or shorter, but under conditions where $\phi = 0.5$ ($k_{21} = k_{23} = 10^8$ s^{-1}), the short pulse limit is 10^{-10}s or shorter (not shown). The 1-μs

laser pulses used in the experiments reported in this paper clearly correspond to the long pulse limit.

DISCUSSION

The data presented in this paper leave little doubt that the flash-induced light saturation curve for the primary photochemistry of photosynthetic reaction centers is exponential in shape. This should not be interpreted to mean that all photosynthetic light saturation curves are exponential. Continuous light experiments, in particular, usually lead to light saturation curves that are not exponential, as has been amply documented (3, 18–19).

Both the Poisson statistical and the kinetic models indicate that in the limit of laser pulses that are long relative to the lifetime of any intermediate transient states and short relative to the overall recombination time of the system, the apparent decay constant of the exponential is easily related to the absolute quantum yield of formation of the photooxidized state. Our results are in excellent agreement with the experiments of Loach and Sekura (8) and Wraight and Clayton (9), who also reported quantum yields of nearly 1.0 for bacteriochlorophyll oxidation in photosynthetic bacteria. A quantum yield of 0.98 is predicted based on available kinetic evidence, because the rate constant for the $P870^+$ $Bpheo^-UQ \rightarrow$ $P870^+BpheoUQ^-$ reaction is $5 \times 10^9 s^{-1}$ (20, 21), while the $P870^+Bpheo^- \rightarrow$ $P870$ $Bpheo$ recombination rate constant is $\sim10^8 s^{-1}$ (22). These rate constants are equivalent to k_{23} and k_{21}, respectively, in the kinetic model.

The $P870^+Bpheo^- \rightarrow$ $P870Bpheo$ recombination is not a simple kinetic process; 10% of the $P870^+Bpheo^-$ centers undergoing recombination decay to a triplet state of $P870$ instead of the ground state (22), and magnetic interactions between $P870^+$ and $Bpheo^-$ influence this process (23). The kinetic model is, therefore, somewhat oversimplified compared with the actual kinetic pathway. This is of no quantitative significance when high quantum yield processes are being measured, but could introduce significant distortion into the light saturation curve if the quantum yield is low, as may be the case in some quinone reconstitution experiments (10, 11). In this situation a pulse significantly longer than the 10–20-μs lifetime of the triplet will again satisfy the long pulse requirement and restore the exponential shape of the curve. In many situations, it may be preferable to measure quantum yields in the short pulse limit since it is unnecessary to record and fit an entire light saturation curve. However, it is necessary to know independently the magnitude of the absorbance change that corresponds to complete conversion. In the intermediate pulse region both the apparent decay constant and the saturation value depend on the pulse duration in a sensitive way.

There is no indication whatever in our data that high intensity pulses cause either an irreversible or reversible loss of photoactivity. The phenomenon of photoinhibition

of photochemistry has recently been observed in flash saturation O_2 yield experiments in *Chlorella* by Ley and Mauzerall (24). Exciton annihilation leading to fluorescence quenching in antenna arrays subjected to intense laser pulses is well documented in photosynthetic systems (25), but it is not clear whether the effect on photochemistry observed by Ley and Mauzerall (24) originates in the antenna or reaction center. The reaction centers used in our experiments contain no antenna. However, the lower absorption cross section, $\sim2A^2$ of our reaction centers compared with $\sim100A^2$ measured by Ley and Mauzerall (24), means that ~50 times more intense pulses would be required to observe the same effect in bacterial reaction centers. After this factor is included, our maximum energy pulses correspond to just where Ley and Mauzerall (24) observed the onset of photoinhibition. Experiments with higher energy pulses or at wavelengths where σ is larger are required to determine if such photoinhibition processes are present in isolated reaction centers.

APPENDIX

Calculation of the Light Intensity Correction Factor

The quantum yield technique described here requires absolute measurements of the light intensity in photons cm^{-2}. The intensity incident on the front surface of the cuvette was measured as described in the Materials and Methods, but the relevant quantity is really the light intensity in the center of the cuvette where ΔA is measured. Therefore, the light intensities must be corrected for reflectivity of the cuvette walls and light absorption by the sample. The calculations described below are adapted from the similar problem treated by Wraight and Clayton (9).

Fig. 3 of reference 9 describes the effects of multiple internal reflections and absorption on the intensity of light in the cuvette. The fraction of light transmitted in one traversal through the sample is t and the fraction of light reflected at the front and rear cuvette walls is r. Values for r were obtained as described by Wraight and Clayton (9); $t = 10^{-A}$, where A is the sample absorbance at the laser wavelength. Typical values for t and r are 0.9 and 0.04, respectively. When the sample absorbance is low, a linear function is sufficient to describe the light intensity decrease across the cuvette, and the intensity at the center of the cuvette on the nth traversal (I_n) of the beam is

$$I_n = \tfrac{1}{2} I_0 (1 + t)(1 - r) t^{n-1} r^{n-1}, \qquad (A1)$$

where I_0 is the incident intensity. The total intensity is the sum of all traversals

$$I = \tfrac{1}{2} I_0 (1 + t)(1 - r) \sum_{i=1}^{\infty} t^{i-1} r^{i-1} \qquad (A2)$$

The series converges to give (26):

$$I = \tfrac{1}{2} I_0 \frac{(1 + t)(1 - r)}{1 - tr}. \qquad (A3)$$

With the typical values quoted above, $I = 0.95 I_0$, so the correction is a small one.

REFERENCES

1. Blackman, F. F., and L. C. Matthaei. 1905. Experimental researches in vegetable assimilation and respiration. IV. A quantitative study of carbon dioxide assimilation and leaf-temperature in natural illumination. *Proc. R. Soc. Lond.* 76B:402–460.
2. Emerson, R., and W. Arnold. 1932. The photochemical reaction in photosynthesis. *J. Gen. Physiol.* 16:191–205.
3. Rabinowitch, E. I. 1951. Photosynthesis and Related Processes. Vol. II. Part 1. John Wiley and Sons, Inc., New York. 964–1082.
4. Mauzerall, D. 1976. Fluorescence and multiple excitations in photosynthetic systems. *J. Phys. Chem.* 80:2306–2309.
5. Mauzerall, D. 1978. Multiple excitations and the yield of chlorophyll a fluorescence in photosynthetic systems. *Photochem. Photobiol.* 28:991–998.
6. Mauzerall, D. 1982. Statistical theory of the effect of multiple excitation in photosynthetic systems. *In* Biological Events Probed by Ultrafast Laser Spectroscopy. R. R. Alfano, editor. Academic Press, Inc., New York. 215–235.
7. Ley, A. C., and D. C. Mauzerall. 1982. Absolute absorption cross sections for photosystem II and the minimum quantum requirement for photosynthesis in *Chlorella vulgaris*. *Biochim. Biophys. Acta.* 680:95–106.
8. Loach, P. A., and D. L. Sekura. 1968. Primary photochemistry and electron transport in *Rhodospirillum rubrum*. *Biochemistry.* 7:2642–2649.
9. Wraight, C. A., and R. K. Clayton. 1973. The absolute quantum efficiency of bacteriochlorophyll photoxidation in reaction centers of *Rhodopseudomonas spheroides*. *Biochim. Biophys. Acta.* 333:246–260.
10. Gunner, M. R., D. M. Tiede, R. C. Prince, and P. L. Dutton. 1982. Quinones as prosthetic groups in membrane electron transfer proteins. I. Systematic replacement of the primary ubiquinone of photochemical reaction centers with other quinones. *In* Function of Quinones in Energy Conserving Systems. B. L. Trumpower, editor. Academic Press, Inc., New York. 265–269.
11. Pocinki, A. G., and R. E. Blankenship. 1982. Kinetics of electron transfer in duroquinone-reconstituted reaction centers from photosynthetic bacteria. *FEBS (Fed. Eur. Biochem. Soc.) Lett.* 147:115–119.
12. Schenck, C. C., R. E. Blankenship, and W. W. Parson. 1982. Radical pair decay kinetics, triplet yields and delayed fluorescence from bacterial reaction centers. *Biochim. Biophys. Acta.* 680:44–59.
13. Straley, S. C., W. W. Parson, D. C. Mauzerall, and R. K. Clayton. 1973. Pigment content and molar extinction coefficients of photochemical reaction centers from *Rhodopseudomonas spheroides*. *Biochim. Biophys. Acta.* 305:597–609.
14. Johnson, L. W., and D. R. Reiss. 1977. Numerical Analysis. Addison-Wesley Publishing Co., Reading, MA. 370.
15. Blankenship, R. E., and W. W. Parson. 1978. The photochemical electron transfer reactions of photosynthetic bacteria and plants. *Annu. Rev. Biochem.* 47:635–653.
16. Bevington, P. R. 1969. Data Reduction and Error Analysis in the Physical Sciences. McGraw-Hill, Inc., New York.
17. Moore, J. W., and R. G. Pearson. 1981. Kinetics and Mechanism, Third ed. John Wiley and Sons, Inc., New York. 455.
18. Jassby, A. D., and T. Platt. 1976. Mathematical formulation of the relationship between photosynthesis and light for phytoplankton. *Limnol. Oceanogr.* 21:540–547.
19. Chalker, B. E. 1980. Modeling light saturation curves for photosynthesis: An exponential function. *J. Theor. Biol.* 84:205–215.
20. Rockley, M. G., M. W. Windsor, R. J. Cogdell, and W. W. Parson. 1975. Picosecond detection of an intermediate in the photochemical reaction of bacterial photosynthesis. *Proc. Natl. Acad. Sci. USA.* 72:2251–2255.
21. Kaufmann, K. J., P. L. Dutton, T. L. Netzel, J. S. Leigh, and P. M. Rentzepis. 1975. Picosecond kinetics of events leading to reaction center bacteriochlorophyll oxidation. *Science (Wash. DC)* 188:1301–1304.
22. Parson, W. W., R. K. Clayton, and R. J. Cogdell. 1975. Excited states of photosynthetic reaction centers at low redox potentials. *Biochim. Biophys. Acta.* 387:265–278.
23. Blankenship, R. E. 1981. Chemically induced magnetic polarization in photosynthetic systems. *Accounts Chem. Res.* 14:163–170.
24. Ley, A. C., and D. C. Mauzerall. 1982. The reversible decline of oxygen flash yields at high flash energies. Evidence for total annihilation of excitations in photosystem II. *Biochim. Biophys. Acta.* 680:174–180.
25. Breton, J., and N. E. Geacintov. 1981. Picosecond fluorescence kinetics and fast energy transfer processes in photosynthetic membranes. *Biochim. Biophys. Acta.* 594:1–32.
26. Dwight, N. B. 1961. Table of Integrals and Other Mathematical Data, Fourth Ed. MacMillan, Inc., New York. 336.